

Evidence for a role in growth and salt resistance of a plasma membrane H⁺-ATPase in the root endodermis

Veronique Vitart^{1,†}, Ivan Baxter¹, Peter Doerner² and Jeffrey F. Harper^{1,*}

¹Department of Cell Biology, The Scripps Research Institute, La Jolla, California 92037, USA, and

²Institute of Cell and Molecular Biology, University of Edinburgh, Edinburgh EH9 3JR, UK

Received 3 April 2001; accepted 26 April 2001.

*For correspondence (fax +1 858 784 9840; e-mail harper@scripps.edu).

[†]Present address: MRC Human Genetics Unit, Western General Hospital, Crewe Road, Edinburgh, UK.

Summary

The plasma membrane of plant cells is energized by an electrochemical gradient produced by P-type H⁺-ATPases (proton pumps). These pumps are encoded by at least 12 genes in *Arabidopsis*. Here we provide evidence that isoform AHA4 contributes to solute transport through the root endodermis. AHA4 is expressed most strongly in the root endodermis and flowers, as suggested by promoter-GUS reporter assays. A disruption of this pump (*aha4-1*) was identified as a T-DNA insertion in the middle of the gene (after VFP₅₇₄). Truncated *aha4-1* transcripts accumulate to approximately 50% of the level observed for AHA4 mRNA in wild-type plants. Plants homozygous for *aha4-1* (–/–) show a subtle reduction in root and shoot growth compared with wild-type plants when grown under normal conditions. However, a mutant phenotype is very clear in plants grown under salt stress (e.g., 75 or 110 mM NaCl). In leaves of mutant plants subjected to Na stress, the ratio of Na to K increased 4–5-fold. Interestingly, the *aha4-1* mutation appears to be semidominant and was only partially complemented by the introduction of additional wild-type copies of AHA4. These results are consistent with the hypothesis that *aha4-1* may produce a dominant negative protein or RNA that partially disrupts the activity of other pumps or functions in the root endodermal tissue, thereby compromising the function of this cell layer in controlling ion homeostasis and nutrient transport.

Keywords: H⁺-ATPase, salt stress, endodermis, *Arabidopsis*.

Introduction

In plants and fungi the major ion pumps in the plasma membrane are P-type H⁺-ATPase (proton pumps) (Morsomme and Boutry, 2000; Portillo, 2000). These pumps function to energize the plasma membrane for nutrient uptake and signal transduction by generating an electrical potential and chemical gradient across the membrane. Biochemical and structural evidence indicates that proton pumps form multimeric structures (Chadwick *et al.*, 1987; Scarborough, 2000). In yeast, one of the two plasma membrane proton pumps, PMA1, is essential, as a null mutation is lethal in haploid cells (Serrano *et al.*, 1986). In plants, it is expected that proton pumps are also essential, although similar analyses have not yet been reported. In addition, small changes in pump activity are thought to be important for many aspects of plant growth and development. For example, many studies have found changes in pump activity in response to a variety of

environmental conditions, including salt stress, hormones, light, and pathogens (Assmann, 1993; Mathieu *et al.*, 1994; Niu *et al.*, 1993; Portillo, 2000).

In *Arabidopsis thaliana*, at least 12 genes predicted to encode plasma membrane H⁺-ATPases have been identified (P-type ATPase Database at <http://biobase.dk/~axe/Patbase.html>). Proton pumps are also encoded by multi-gene families of unknown size in tobacco (Boutry *et al.*, 1989; Moriau *et al.*, 1993) and tomato (Ewing *et al.*, 1990). To date, a unique function has not been ascribed to any of the multiple isoforms in *Arabidopsis*. However, it is clear that many of the isoforms have tissue-specific patterns of expression, different enzyme kinetics, and differences in their autoinhibitory domain, which may result in different regulatory properties (Harper *et al.*, 1994; Luo *et al.*, 1999; Michelet and Boutry, 1995; Moriau *et al.*, 1999; Palmgren and Christensen, 1994). In tobacco, the cosuppression of at

least one H⁺-ATPase resulting from the attempted over-expression of isoform PMA4 resulted in pleiotropic effects on sucrose translocation, stomatal opening, growth, and fertility (Zhao *et al.*, 2000). To better characterize the function of individual members of this gene family in *Arabidopsis*, a systematic screen to identify proton pump gene disruptions was initiated (Krysan *et al.*, 1996). This work indicated that at least some mutants are viable with proton pump gene disruptions, but no phenotypes were reported.

Here we report the mutation *aha4-1* resulting from a T-DNA insertion in the *Arabidopsis* proton pump isoform *AHA4*. We provide evidence that *AHA4* contributes to solute transport through the root endodermis. The *aha4-1* mutation results in plants with greatly increased sensitivity to salt stress. Interestingly, *aha4-1* appears to be semi-dominant and was only partially complemented by the introduction of additional wild-type copies of *AHA4*. We further show that this plant line accumulates several truncated *AHA4* mRNAs, one of which potentially leads to a truncated protein with a poly-lysine C-terminal end. Consistent with dominant proton pump mutations in yeast, we present a speculation that the *aha4-1* disruption may give rise to a defective pump that partially disrupts the activity of other pumps, possibly by interfering with biogenesis or stability of multimeric pump complexes.

Results

Cloning of H⁺-ATPase isoform *AHA4*

AHA4 was first identified as a short PCR fragment in an experiment aiming to identify all members of the *Arabidopsis* H⁺-ATPase family (Harper *et al.*, 1994). We subsequently isolated a full-length genomic clone (Figure 1) and sequenced the entire coding region. DNA sequence analysis indicated a 100% identity to a proton pump gene recently identified by the genome sequencing project on chromosome 3 (At3g47950, BAC clone T17F15).

Analysis of the current plant protein database revealed that *AHA4* is most closely related to an *Arabidopsis* plasma membrane H⁺-ATPase, which was previously cloned and identified as *AHA11* (J.F. Harper, unpublished). These two H⁺-ATPases isoforms are more closely related to the 'PMA1' group of tobacco H⁺-ATPases than to previously characterized *Arabidopsis* *AHA1*, 2, 3, 9, and 10 (Figure 1a). *AHA4* shows the highest similarity (90%) to tobacco PMA1, but only 80% similarity to the *Arabidopsis* *AHA2*. Therefore, *AHA4* and its closest relative *AHA11* define a third distinct subgroup within the *Arabidopsis* plasma membrane H⁺-ATPase family, with the other two branches defined by *AHA10* alone and the group of *AHA1*, 2, 3, 9, respectively.

AHA4 is expressed primarily in the root endodermis

To gain insight into the tissue-specific pattern of *AHA4* expression, the β-glucuronidase (GUS) reporter was placed downstream of the *AHA4* promoter in a translational fusion and transformed into plants. A total of 10 independent transgenic plant lines were analyzed; all displayed a very similar pattern of GUS activity with variations in intensity. GUS staining was the strongest in roots, hypocotyls, and flowers of transgenic plants (Figure 2). Very little activity was detected in excised cotyledons and leaves. Strong staining was observed in the emerging root tip in germinating and 2-d-old seedlings, as well as in internal cell layer(s) of maturing and differentiated root tissues (Figure 2c,d,e). In seedlings older than 1 wk, staining was no longer detectable within tissues of the meristematic and elongation zone, but was restricted to internal cell layer(s) of the differentiated root and the hypocotyl (Figure 2c). The root-hypocotyl junction stained particularly strongly. In mature plants, GUS activity was also detected in siliques and flowers. In siliques, staining was observed in the basal and apical tissues as well as in the conductive tissue and the seed coat (Figure 2b). In flowers, staining was highly variable, even in flowers of the same plant at similar developmental stages (Figure 2a). Staining was normally strongest in anther filaments, maturing pollen grains, and stigma.

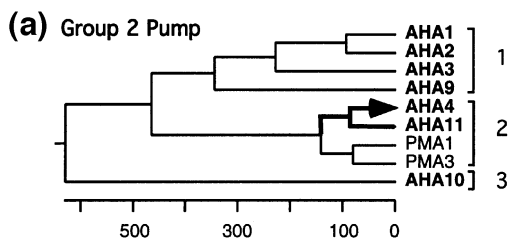
Since the root showed the strongest consistent staining, this tissue was further analyzed in 1-wk-old seedlings. Cross-sections of differentiated tissues of GUS-stained roots revealed the strongest staining in the endodermis (Figure 2e), while lighter and more variable staining was observed in the parenchyma cells of the stele. The epidermal, cortical, and phloem cells showed no detectable staining.

To verify the organ-specific expression pattern we compared the GUS reporter results with relative abundance of *AHA4* transcripts detected in different tissues by a quantitative RT-PCR analysis. Consistent with the pattern of GUS activity, 5-wk-old plants showed 26–37-fold more transcript in roots than stem or leaf tissues (Table 1).

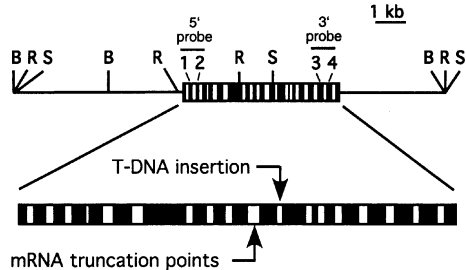
Identification of a T-DNA disruption, *aha4-1*

The *aha4-1* T-DNA disruption was fortuitously identified in a plant line being analyzed for a terminal flower phenotype. A genomic fragment containing the border between the 5' side of the pump gene and the T-DNA was cloned (clone λ-8) and the region containing the T-DNA border sequenced (Figure 1c). The T-DNA was found to disrupt the gene within the 11th predicted intron. Plant lines containing only a single T-DNA insertion were generated through a series of three backcrosses. Southern blot analyses of backcrossed lines indicated a single insertion.

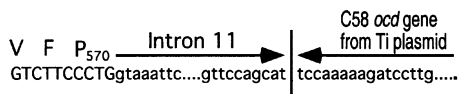
However, the inserted T-DNA itself was found to be rearranged, as the expected size fragments for a restriction digest of the T-DNA were not observed (data not shown). Nevertheless, a Southern blot and PCR analysis confirmed that the 3' end of *AHA4* gene was still present downstream of the insertion site (data not shown), thereby confirming that downstream sequences were not deleted. Thus the T-DNA insertion appeared to cleanly disrupt the coding sequence at a position corresponding to the middle of the ATPase catalytic domain (between the conserved CSDK and GDGV sequences).



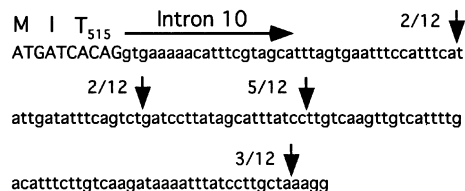
(a) Group 2 Pump



(b) *AHA4* wild type, Lambda 3.5 insert



(d) mRNA truncation points



(e) Predicted C-termini of truncated proteins

- 1)...MITG₅₁₆/EKHFVAFSEFPFQK.....(K)ⁿ*
- 2)...MITG₅₁₆/EKHFVAFSEFPFHIDISV*

A truncated AHA4 mRNA is expressed in the aha4-1 mutant

To examine whether *aha4-1* plants accumulated a truncated mRNA, we compared mRNA from Col-0 and *aha4-1* plant tissues using a semiquantitative RT-PCR analysis (Figure 3). An RT-PCR analysis was necessary since the endogenous transcript was not abundant enough to be detected in a standard RNA blot analysis (Northern). Using PCR primers specific to the 3' end of *AHA4*, an RT-PCR product of the expected size was generated from Col-0 RNA but not from *aha4-1* RNA. Amplification of the elongation initiation factor 4 α -2 gene (*eIF4 α*), as an internal control, indicated the presence of similar initial amounts of intact cDNA templates in both Col-0 and *aha4-1* plant tissue extracts. No amplification of contaminating genomic sequence could be detected. The absence of an *AHA4* 3' product in the mutant line is consistent with the expectation that the large T-DNA insert disrupted a tran-

Figure 1. Diagrams showing the relationship of *AHA4* related proton pumps, and the T-DNA insertion site in *aha4-1*.

(a) Distance tree showing the three major groups of characterized plant H⁺-ATPases. Protein sequences were compared by MegAlign Software using J. Hein method with PAM250 residue weight table. PMA1 and PMA3 are *Nicotiana plumbaginifolia* H⁺-ATPases isoforms 1 and 3 (accession numbers sp./Q08435 and sp./Q08436). All 'AHA' sequences are from *Arabidopsis thaliana* H⁺-ATPases. *AHA4* and *AHA11* (accession number BAA97214) were deduced from genomic sequences determined from clones isolated in the Harper laboratory. *AHA4* was found to be identical to a predicted H⁺-ATPase sequence encoded by BAC 17F15 (accession number pir/T06688) except at position 572–574 where the database predicted protein sequence of 'FSA' instead of 'VFP'. Since the VFP sequence is very conserved in other H⁺-ATPases, we believe our interpretation of an alternative splice site leading to a VFP prediction is correct. *AHA1*, 2, 3, 9, and 10 are characterized H⁺-ATPases (accession numbers sp./P20649/PMA1ARATH, sp./P19456/PMA2ARATH, sp./P20431/PMA3ARATH, pir//S60301 and GI:765353)

(b) Diagram of *AHA4* and its flanking regions. The 8 kb insert is shown for a lambda clone (λ 3.5) containing *AHA4*. *AHA4* exons and introns are represented by black and white boxes, respectively. B, BamHI; R, EcoRI; S, SacI. Points 1, 2, 3, and 4 indicate the positions of primers used in Figure 3 to evaluate transcription and probe for 5' and 3' ends of the gene.

(c) DNA sequence of the T-DNA insertion site in the *AHA4* gene. The T-DNA inserted within intron 11, producing an antisense fusion with the Ti plasmid's *ocd* gene.

(d) The mRNA truncation points. Four different truncation points were identified (arrows with numbers indicating frequency observed) in intron 10, upstream of the T-DNA insertion site located in intron 11. Sequence was determined for 12 examples of cloned 3' ends. PCR amplification from 1st strand cDNA was conducted using an oligo-dT primer for the 3' end, and three nested *AHA4* primers from exons 8 and 9 (Primers 202, GAGCAAAGGTGCTCCTGAGC; 426a, GCGGAGAGTTCATGCTGTTATTG; 426b, AAACCTCGAGTCGCTGAAAGGGGTCTG). All clones showed correct splicing of intron 9, which verified that the products were derived from cDNA and not genomic DNA.

(e) Predicted C-termini of truncated *aha4-1* gene product. The four different truncation points result in at least two different predicted termini. Example one (most upstream truncation point) results from an open reading frame extending into the poly A tail. The number of C-terminal lysines (Kn) may vary depending on the length of the poly A tail.

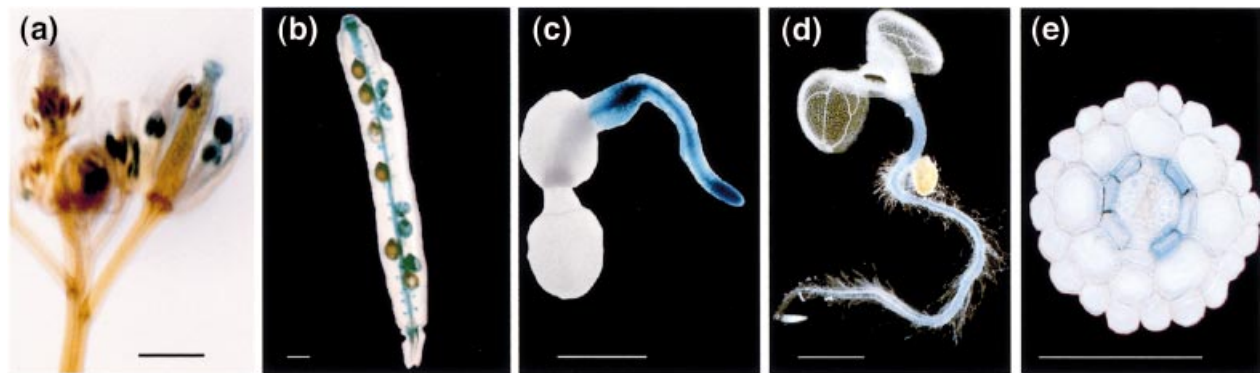


Figure 2. Cell and tissue specific expression of *AHA4* based on a GUS-reporter assay. Histochemical localization of GUS was conducted with transgenic plants containing a promoter-*AHA4*::*GUS* construct. Blue staining indicates GUS activity.

- (a) Flowers. 4 h staining reaction
 (b) Maturing silique. 4 h staining reaction.
 (c) 2-d-old seedling. 2 h staining reaction
 (d) 1-wk-old seedling. 4.5 h staining reaction
 (e) Cross-section through upper root of a 1-wk-old seedling. 3.5 h staining reaction.
 Scale bar = 1 mm in a, b, c, and d, 100 μ m in e.

Table 1. *AHA4* expression pattern in 5-week-old *Arabidopsis* plants based on RT-PCR performed on Col-0 ecotype and GUS activity assays performed on *Arabidopsis* expressing a *AHA4* promoter::*GUS* fusion

organ	<i>AHA4</i> mRNA levels based on RT-PCR: Normalized expression level		GUS activity normalized to leaf GUS level
	relative to <i>eIF4α</i>	relative to <i>UBQ10</i>	
flower	37	33	30
stem	1	2	1.3
leaf	1	1	1
root	37	26	330

Arabidopsis plants were grown 5 wk in Magenta boxes on 0.5X MS, 2% sucrose. Levels of mRNA were normalized to *eIF4 α* or *UBQ10* level and then to expression levels found in leaves. GUS activity of extracts from four independent transformants expressing *AHA4*::*GUS* fusions were measured by fluorometric assay and expressed as pmoles MUG $\text{min}^{-1} \mu\text{g}^{-1}$ protein.

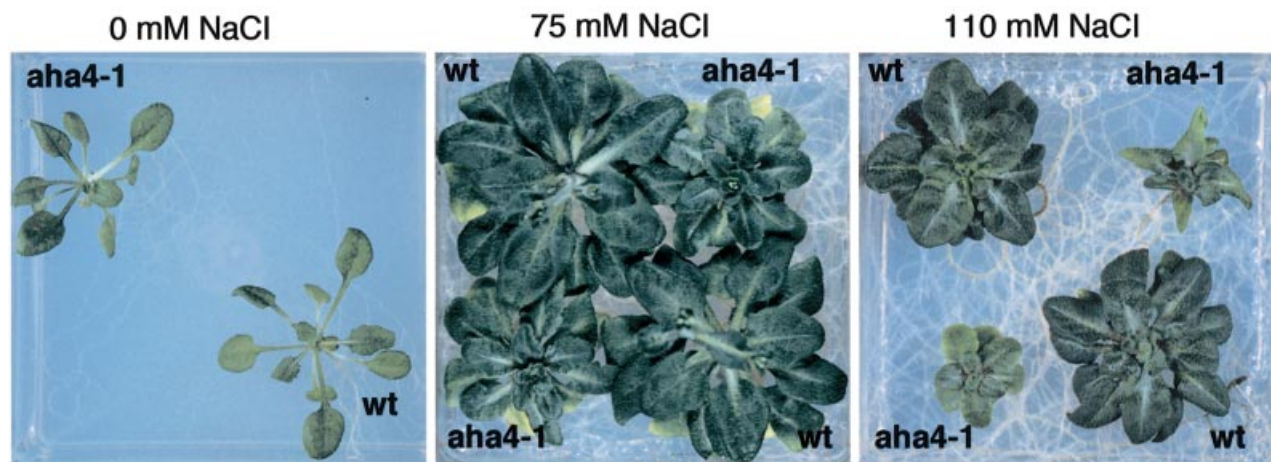


Figure 4. Mutant *aha4-1* plants have increased sensitivity to salt stress.

Four-day-old wild-type and *aha4-1* seedlings grown on GM media were transferred to Magenta box containers with germination media supplemented with 0 mM additional NaCl, 75 mM NaCl, or 110 mM NaCl. The plants were photographed after 2 wk (0 mM NaCl) or 5 wk (75 and 110 mM NaCl).

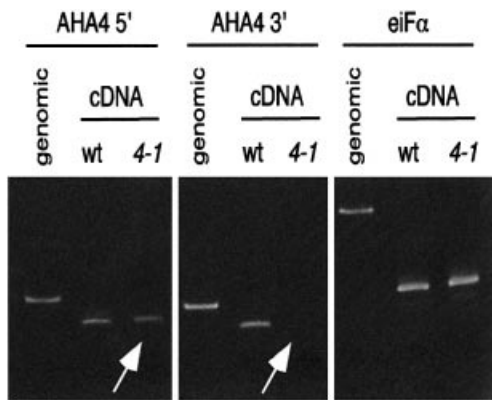


Figure 3. RT-PCR showing that *aha4-1* plants express a truncated *AHA4* transcript.

cDNA templates were generated by reverse transcription of either wild type Col-O (wt) or *aha4-1* mutant (4-1) total RNA using oligo-dT as a primer. Subsequent PCR reactions were used to amplify sequences lying upstream of the T-DNA truncation point (*AHA4* 5'; primer pair 67-82cd; sites 1 and 2 in Figure 1b) and downstream of it (*AHA4* 3'; primer pair 139c-144b, sites 3 and 4 in Figure 1b). As a control for the quality of the template, PCR amplifications were also done in parallel for sequences corresponding to the housekeeping gene coding for the initiation factor 4 α -2 (*eIF4 α -2*; primer pair *eIF4 α u* and *eIF4 α d*). The corresponding products were run on a 5% acrylamide gel in lanes noted *AHA4* 5', *AHA4* 3', and *eIF α* , respectively. Lanes marked 'genomic' are control reactions in which the same primer pairs were used to amplify genomic DNA. The genomic products all contain intron sequences and are therefore larger, confirming that the smaller cDNA products originated from mRNA. Arrows point to the band positions expected for the 5' and 3' ends of *AHA4* cDNA. Note the presence of a 5' end amplification product using the *aha4-1* plant template, but the absence of a corresponding 3' end amplification product, as expected for a truncated *aha4-1*.

scriptional read-through into the 3' end of the gene. In contrast, using PCR primers specific for the 5' end of *AHA4*, a parallel RT-PCR reaction showed a product for both the wild-type and *aha4-1* mutant, although RNA abundance in the mutant was about 2-fold lower than in the wild type (Figure 3). To confirm that this product corresponded to isoform *AHA4* and not to its most closely related isoform, *AHA11*, a second set of 5' primers was used to amplify a 1.02-kb 5' product, which included a diagnostic MfeI restriction site unique to the *AHA4* isoform. This set of primers exclusively amplified the *AHA4* RT-PCR product in Col-0 and *aha4-1* plant tissue extracts, as diagnosed by a complete digestion at the MfeI site, and again with an approximate ratio of 2:1 (data not shown). Taken together, these results indicated that a truncated *AHA4* transcript accumulates to significant levels in *aha4-1* plants.

Given the presence of truncated *aha4-1* mRNA, it seems likely that the cellular machinery would attempt to translate this mRNA into a truncated protein. To determine possible C-terminal ends of truncated proteins, we cloned and sequenced the 3' ends of truncated *aha4-1* mRNAs. The mRNA truncation points were determined for 12 clones obtained from PCR amplification of 1st strand

cDNA using oligo-dT as a 3' end primer and three nested *AHA4* upstream primers. From these 12 representative clones, four different truncation points were found (Figure 1d). Interestingly, all these points were located in intron 10, considerably upstream from the T-DNA insertion site located in intron 11. From these representative truncations, at least two different *aha4-1* protein products were predicted, one of which may contain a long stretch of lysines resulting from translation into the poly A tail (Figure 1e, example 1).

Phenotype of the *aha4-1* mutant

To test for a potential phenotype resulting from the *aha4-1* mutation, the growth and development of wild-type and mutant plants were compared side by side under axenic conditions throughout the life cycle (Table 2). Vegetative development was evaluated by (1) measuring root growth during the first several weeks after germination; (2) scoring the number of days from germination to floral initiation; and (3) determining the DW and number of leaves in the rosette at the time of floral initiation. While a growth phenotype was observed for roots and rosettes, floral morphology and fecundity appeared to be unaffected (not shown).

Root phenotype. Since *AHA4* was found to be expressed at high levels in the root, we compared the growth rate of roots from wild-type and mutant plants grown side by side on the surface of an agar plate containing normal growth media (0 mM added NaCl), or media supplemented with 75 mM NaCl (mild salt stress). At 0 mM added Na, *aha4-1* roots showed a 20% reduction in growth compared with wild-type plants, as determined by the length of the primary root after 12 d of growth. A similar 20% difference was observed for roots growing on 75 mM NaCl, although longer growth periods (e.g., 20 d) eventually lead to a 30% difference (not shown).

To examine the cellular basis for this observation, the length of individual cortical cells was measured in roots from wild-type and mutant plants using a light microscope and Nomarski optics. Cortical cells from the *aha4-1* mutant were 10% shorter (*t*-test, $P < 0.01$). A total of more than 500 cells for each plant line were measured in three independent experiments. The average length of cells from wild-type and *aha4-1* roots was 220 and 198 μ m, respectively. A similar 10% decrease in cell length was also observed for plants grown in 75 mM salt. Thus, the 'short root phenotype' can be partially accounted for by a reduction in cell size.

Rosette phenotype. The most severe phenotypic affect was observed in the rosettes, even though *AHA4* was not strongly expressed in that tissue. Under normal growth

Table 2. Quantitative differences between Col-0 and *aha4-1* mutant plants when grown under normal and 75 mM NaCl stress conditions

	Root growth at 12 d (length, cm)		Leaf no. at time of floral initiation		Rosette mass (mg) at time of floral initiation		Days to floral initiation	
	0	75 mM	0	75 mM	0	75 mM	0	75 mM
wt. (Col-0)	12.5 ± 1.1	7.1 ± 1	21.1 ± 2.6	21.1 ± 2.6	6.8 ± 2.1	26.1 ± 7.6	24 ± 1.4	42.2 ± 6.3
<i>aha4-1</i>	10.1 ± 1.1	5.6 ± 0.8	18.6 ± 2.4	18.6 ± 2.4	4.8 ± 1.3	16.7 ± 3.6	24.6 ± 2.2	46.8 ± 5
Difference: (<i>t</i> -test <i>P</i> < 0.01)	- 19%	- 18%	0	- 12%	- 29%	- 36%	0	11%

conditions the rosettes from the *aha4-1* mutant were smaller (29% less mass) than the wild type, although leaf number and time to flowering were equivalent. However, under a mild 75 mM salt stress, the growth difference was further increased to 36%, and plants produced 12% fewer leaves and flowering time was delayed by 11%.

When grown in the presence of 110 mM NaCl (severe salt stress), the difference in vigor between the two genotypes was very dramatic and was easily scored after a 5-wk growth period (Figure 4). In our standard assay, two wild-type and two mutant plants were grown in the same container (a total of 16 mutant plants in eight boxes). In each container, the two mutant lines always exhibited a clear growth reduction compared with wild-type controls. This phenotype did not result from a specific ionic stress, as similar growth differences were also observed with media containing 110 mM KCl, 55 mM Na₂SO₄, or 110 mM NaNO₃ (data not shown). These results suggest that the increased salt sensitivity of rosette growth in the *aha4-1* mutant could be caused by a general defect in the ability to handle high ion stress.

More Na accumulates in leaves of aha4-1 plants grown under salt stress

To gain insight into how a rosette growth phenotype could be caused by a defective pump expressed primarily in root and reproductive tissues, we evaluated the ion composition of leaf material from plants subjected to salt stress for evidence of perturbation in ion homeostasis. The relative accumulation of K, Na, Ca, P, and Mg was determined by ICP-AES (Inductively Coupled Plasma-Atomic Emission Spectroscopy) on leaves from 24-d-old Col-0 and *aha4-1* plants grown on media supplemented with 75 mM NaCl. This analysis revealed higher levels of Na and lower levels of K in leaves from the mutant plants, while relative levels of Mg, P, and Ca remained similar (Figure 5). This perturbation in Na/K homeostasis was easily seen in the ratio of K to Na, which showed a dramatic 4–5-fold

difference between genotypes. These results suggest that the *aha4-1* plants were compromised in their ability to exclude Na, when challenged with a mild NaCl stress.

The aha4-1 mutation is semidominant

To demonstrate that the T-DNA insertion in the *AHA4* gene was causally related to the observed phenotype, we first examined the linkage between the *aha4-1* mutation and the salt sensitive phenotype, and subsequently attempted to complement a homozygous *aha4-1* mutation by the introduction of wild-type copies of *AHA4*.

The salt sensitive phenotype was observed in two independently back-crossed homozygous lines, *aha4-1* (H) and (E), each generated after three back-crosses to a wild-type Col-0 parent. To further evaluate the apparent linkage and determine the strength of the *aha4-1* mutation, the phenotype of 38 heterozygous F1 plants resulting from crosses between an *aha4-1* plant (–/–) (H line) and Col-0 were examined. All 38 heterozygotes had intermediate or severe salt sensitive phenotypes, as scored visually and quantitatively at the onset of flowering with plants grown on 75 mM NaCl (e.g., their average FW was 22.7 mg compared with 26 mg for wild-type and 17 mg for homozygous *aha4-1*). This result suggested that the *aha4-1* mutation was semidominant.

Co-segregation of the *aha4-1* allele and the severity of salt sensitivity was then examined in 217 randomly selected F2 seedlings transferred to media supplemented with 110 mM NaCl (four plants per container). Five weeks after their transfer, plants were scored as large, intermediate, or small. The genotypes of all plants were determined by PCR using *AHA4* and *aha4-1*-specific primer pairs. All plants scored as large (48 out of 217) were identified as wild type, while all plants scored as intermediate or small were identified as heterozygous or homozygous for *aha4-1*. These results again supported a tight linkage (within 0.25 map units) between the salt sensitive phenotype and the *aha4-1* T-DNA insertion.

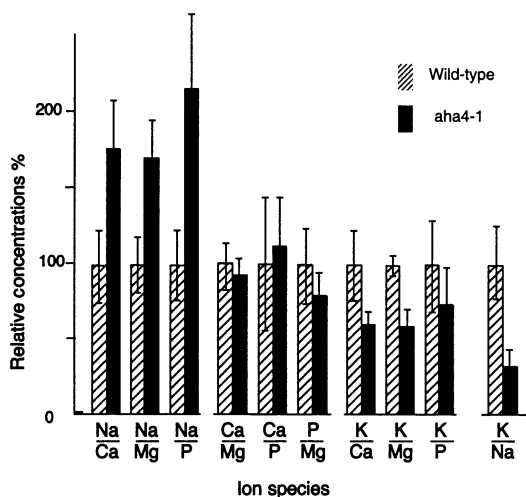


Figure 5. Mineral nutrient analysis shows an increased Na accumulation in *aha4-1* plants.

Elements were measured by ICP-AES in samples of leaves from wild-type and *aha4-1* plants 20 d after transfer to media containing 75 mM NaCl. Values are means \pm standard error of eight independent samples normalized to wild-type as 100%. Note that the accumulation of Na relative to either Ca, Mg, or P is increased in the *aha4-1* mutant compared to wild-type plants. As a control, the relative ratios between Ca, Mg, and P were shown to be equivalent between mutant and wild-type.

Further evidence for the semidominant nature of the *aha4-1* mutation came from our attempts to complement the salt sensitive phenotype with additional wild-type copies of *AHA4*. Homozygous *aha4-1* plants were transformed with a construct carrying the *AHA4* gene under its own promoter and a gene conferring resistance to BASTA™ as transformation marker. Of 27 independently transformed plant lines, 21 were determined to carry multiple insertions of the wild-type *AHA4* gene (the other six had single copy insertions), as determined by segregation analysis of the BASTA marker. The salt sensitivity phenotype was scored in T2 progeny (at least four plants for each of the 27 lines) after 5 wk of growth on media containing 110 mM NaCl. From this survey, only two plant lines showed a significant restoration of salt resistance compared with the untransformed or vector only transformed controls. Significantly, these two lines showed intermediate phenotypes suggesting only partial complementation. These intermediate phenotypes were confirmed in two independent growth experiments and examined in more detail for progeny of line E2-C-B14. Using representative plants grown on 110 mM NaCl, the ratio of K:Na in leaf material was determined by an ICP-AES analysis. The K:Na ratio was intermediate between *aha4-1* ($-/-$) plants and wild-type (complementation line = 34, with *aha4-1* ($-/-$) plants at 16 and wild-type at 100). This intermediate K:Na is consistent with *aha4-1* being semidominant.

Discussion

A conditional phenotype under stress

The analysis here of mutant *aha4-1* provides the first characterization in plants of a mutation in a P-type H^+ -ATPase. At the onset of these experiments, the expression of multiple proton pump isoforms in largely overlapping patterns was expected to provide some level of redundancy, such that the absence of one isoform would be compensated by the presence of another. Nevertheless, two phenotypes were observed in the *aha4-1* mutant. First, there was a modest growth reduction in roots and rosettes under 'normal' growth conditions (Table 2). Second, there was a conditional phenotype observed as a dramatic decrease in rosette growth in response to a general salt stress. This salt-sensitive phenotype was clearly evident when *aha4-1* plants were grown on media containing 110 mM NaCl (Figure 4).

In contrast to expectations for most T-DNA disruptions, *aha4-1* was found to be a semidominant as opposed to a recessive null mutation. This raises the possibility that the observed phenotypes resulted from as little as a 50% reduction in the level of *AHA4* pump (e.g., as expected from a heterozygote with only one functional copy of *AHA4*), or that the *aha4-1* gene product functions as a dominant negative that affects other proton pump isoforms or other processes. While these alternative hypotheses prevent us from concluding a specific role for *AHA4* in salt resistance, the following discussion strongly favors the hypothesis that a defect in proton pumping activity is a reasonable explanation for the phenotypes observed.

There is precedence from yeast for a defect in proton pumping resulting in a conditional phenotype. In *Saccharomyces cerevisiae*, *pma1* mutants with only 33% of wild type proton-ATPase activity still display the same growth rate as the wild-type when the media is above pH 5.5, but dramatically reduce their growth rate as pH is further decreased (Vallejo and Serrano, 1989). Similarly, the *Arabidopsis* mutant 5-2, initially isolated for its resistance to fusicoccin, displayed reduced H^+ -ATPase activity that correlated with a conditional growth phenotype in high light stress conditions (De Michelis *et al.*, 1996; Marre *et al.*, 1995). These observations suggest that under various stress conditions, reduced levels of proton ATPase activity can severely impair cellular functions.

In plants, salt resistance is thought to depend on an increase in proton pump activity. For example, the exposure of plants to high external NaCl results in hyper-osmotic stress, ionic imbalance and Na^+/Cl^- toxicity (Serrano, 1996). To alleviate Na^+/Cl^- toxicity and re-establish cellular ion homeostasis, transport processes across the plasma membrane involving proton pumps are necessary (e.g., Na-antiporters) (Niu *et al.*, 1995). In tobacco cell cultures,

post-transcriptional modification of H⁺-ATPases following salt stress has been reported, resulting in increased affinity for ATP (Reuveni *et al.*, 1993). In whole tobacco and *A. nummularia* plants, NaCl-stress enhanced H⁺-ATPase mRNA accumulation in roots and expanded leaves (Niu *et al.*, 1993). In *A. nummularia* roots the pump mRNA was shown to accumulate to high levels in the epidermis of the root tip and the endodermis of the elongation/differentiation zone, suggesting that increased pump activity specifically in these tissues may be important for the salt stress response (Niu *et al.*, 1996).

Evidence presented here is consistent with the simple hypothesis that the *aha4-1* mutation results in a reduced capacity to pump protons and hence to maintain the electrochemical gradient across the plasma membrane in those cell types that normally express AHA4. Since AHA4 appears to be strongly expressed in the root endodermis (Figure 2), and this tissue has been implicated in the salt stress response in other species, our favored hypothesis is focused on the potential effects of reduced pump capacity in root endodermal cells.

The endodermis provides a barrier to apoplastic transport between the root surface and the vascular bundle. All nutrients carried by the vascular system must therefore pass symplastically through this cell layer on their way to the shoot. Pronounced differences in ionic composition have been observed in endodermal cells when compared with adjacent cell types of the root. For example, in barley roots, measurements of K/Na distribution in cortical, endodermal, and stele cells using X-ray microanalysis showed that the endodermis acts as an efficient barrier to Na (Pitman *et al.*, 1981). If, like in barley, the *Arabidopsis* endodermis creates a selective barrier for Na loading into the conductive tissues and therefore its further transport to the shoot, our data showing relative increases in Na content of leaves from mutant plants grown under Na-stress is consistent with a defect in the endodermal cell functions of *aha4-1* plants. We also observed a stress phenotype with 110 mM K⁺ ions. Thus, it appears that the salt stress phenotype is not a direct response to Na toxicity, but rather reflects a general impairment of membrane transport activities associated with the endodermis.

While the hypothesis above explains how a mutation of a root pump can cause a rosette growth phenotype, it is interesting that despite the apparent strong expression of AHA4 mRNA in some reproductive tissues, there was no detectable phenotype in floral development and fecundity. The low penetrance of the *aha4-1* mutation in these tissues may be due to high levels of other proton pump isoforms, or cell-type specific factors that suppress the ability of the *aha4-1* gene product to function as a dominant negative protein or mRNA.

A mechanism by which aha4-1 may function as dominant negative

Two lines of genetic evidence support the hypothesis that *aha4-1* is dominant or semidominant. First, the severity of phenotype observed in *aha4-1* heterozygotes was typically the same or half that observed in the homozygote. Second, the *aha4-1* mutation was only partially complemented by extra copies of an AHA4 transgene, and this partial complementation was only observed at a low frequency (2 of 27).

While the two examples of partial complementation support the hypothesis that the mutant phenotype results from a competition between wild-type and mutant gene products, we expected a greater complementation frequency since most heterozygotes showed intermediate salt stress phenotypes. The failure to see a higher complementation frequency has at least two potential explanations. First, in many cases transgenes fail to express at the same level or with the same regulatory controls as the endogenous genes, due either to variation in sites of chromosome integration or absence of upstream or downstream regulatory controls. Since our AHA4 transgene was introduced as an 8-kb genomic fragment, some upstream or downstream elements may be missing, such as an enhancer that would respond to salt stress and allow the wild-type transgene to compete with a possible stress induction of the mutant gene. Second, phenotype penetrance and gene dosage may not be directly proportional. For example, while a dose of one mutant gene may 'poison' 10% of the H⁺-ATPase complexes, a dose of two mutant genes may have an even greater than 2-fold increased effect. Thus, complementation of a genotype with two mutant gene copies may require much more than the simple addition of one or two extra copies of a wild-type transgene. Regardless, the low frequency of complementation suggests that in most cases transformation of *aha4-1* (-/-) with extra copies of our AHA4 transgene did not recreate a situation equivalent to a heterozygote in which one copy of the mutant allele was partially compensated by one copy of a wild-type AHA4.

At present, the mechanism by which *aha4-1* creates a dominant phenotype is unclear. While it is possible that the truncated mRNA itself could have a negative effect (e.g., gives rise to suppression of other pump genes), we favor the speculation that a truncated protein functions as a dominant negative. Although T-DNA insertions often produce unstable truncated mRNAs, stable RNA products are certainly possible, as observed for a T-DNA disruption of a putative anion channel (Geelen *et al.*, 2000). In the case of *aha4-1*, we observed that a truncated mRNA accumulated to nearly the same levels as wild-type mRNA. An analysis of the 3' end of these truncated products revealed at least four different truncation points, giving rise to the

possibility of at least two different proteins, one of which would have a poly-lysine C-terminal end resulting from an open reading frame that extended into a poly-A tail. Whether one or more of these truncated proteins has a dominant negative effect in plants is not known. However, in yeast there is evidence that aberrant pumps can act as dominant negatives. Several dominant lethal proton pump mutations have been reported (Maldonado *et al.*, 1998; Portillo, 1997). In some cases, expression of the mutant protein has been shown to block the targeting of wild-type pump to the plasma membrane, presumably through integrating into a multimeric pump complex and causing it to be retained in the ER. In theory, such 'defective complexes' may also be more sensitive to proteolytic destruction and be destroyed more rapidly at any point along the secretory pathway. Therefore, by analogy to yeast, we favor the speculation that the *aha4-1* gene product may function as a dominant negative protein in plant cells by interfering with the transport or stability of a multimeric H^+ -ATPase complex.

Conclusion

Results from our analysis of the *aha4-1* mutant provide the first demonstration in plants of a phenotype associated with a mutation in a proton pump gene. The semidominant nature of *aha4-1* suggests that the resulting gene product may provide a dominant interfering mRNA or protein that can be used to reduce pump activity. Given the expectation in *Arabidopsis* that multiple proton pump isoforms provide redundant functions in most cell types, the development of a dominant negative transgene is worth considering as a powerful genetic strategy along with standard gene knockouts to evaluate the aggregate function of proton pumping in selected cell types.

Experimental procedures

Plant material and genetic analysis

The *aha4-1* mutant line was identified in a population of *Arabidopsis thaliana* ecotype Columbia (Col-0) plants transformed with a T-DNA construct derived from the vector pMON530. This population was screened for mutant flower phenotypes. However, the floral phenotype that prompted the analysis of *aha4-1* plant line was subsequently shown to be unlinked to the pump mutation. During back-crosses, resistance to kanamycin (T-DNA marker) and the floral phenotype were scored phenotypically in individual plants and the disrupted *AHA4* gene was monitored molecularly. A 484-bp PCR product generated by the *AHA4* primer 195, 5'-GATCCGCCTAGGC-ATGACAG-3' and the T-DNA specific primer 71b, 5'-CACAGCAGCCCACTCGACC-3' was diagnostic for the disrupted *AHA4* allele. Segregation patterns of these three characters showed that the original T1 plant contained more than one T-DNA and that its floral phenotype was unlinked to any T-DNA.

Homozygous lines containing only one T-DNA copy (assessed by kanamycin resistance) linked to the *AHA4* disrupted gene were identified from two independent series of three back-crosses followed by two generations of selfing and called *aha4-1* mutant (H) and (E). These two lines, maintained by selfing, were used in all subsequent experiments. Crossing homozygous *aha4-1* mutant (H) plants with Col-0 wild-type plants generated plants heterozygous for the *aha4-1* mutation. F2 populations were generated by selfing heterozygous plants.

Genomic clones

The genomic clone λ 8 encompassing the *aha4-1* allele was isolated by screening a λ GEM11 genomic library constructed with DNA from the T1 transgenic plant exhibiting the floral phenotype with a T-DNA specific probe. The genomic clone λ 3-5 containing the *AHA4* gene was isolated from an *Arabidopsis thaliana* λ GEM11 genomic library (R. Mulligan). This library was probed with a 290-bp genomic fragment generated by PCR primers 82 u, 5'-GTTCTACTACTATGCTTTCA-3' and 82cd 5'-TTACTCCTCCATT-AGCAAGCGC-3'. The BamHI fragment from clone λ 3-5 was subcloned into pBluescript SK⁻ (Stratagene, La Jolla, CA, USA) and called p74. This clone was used as template to sequence *AHA4* on both strands. DNA sequences were determined by a dye-primer sequencing method on a DNA sequencer at the core facility at the Scripps Research Institute, CA, USA. Sequence similarities were calculated using the MegAlign software (DNASTar, Madison, WI, USA).

Growth conditions

Surface sterilized seeds were plated on germination media (GM) (0.5x Murashige and Skoog salts (Sigma, St Louis, MO, USA), 0.5 g l⁻¹ Mes (Sigma), 2% sucrose, pH 5.7 adjusted with KOH). The plates were stored at 4°C in the dark for 48 h and then placed in a vertical orientation in a growth chamber (22°C, continuous white light). After 4 d, seedlings at the same developmental stage were transferred to appropriate plates or Magenta boxes (Sigma). For all other purposes, seedlings were grown 2 wk on germination plates, transferred to soil (Metro-Mix; Grace Sierra Horticultural Products Co., Milpitas, CA) and placed in a growth room (20°C, continuous light).

Growth measurements

For root elongation comparisons, root-bending assays (Wu *et al.*, 1996) were performed. Twelve healthy 4-d-old seedlings, six Col-0 and six *aha4-1* plants, were transferred along one line of a vertically oriented test plate. Test plates were large round plates (15 cm of diameter) of GM media alone or supplemented with 75 mM NaCl. After 1-3 d, plates were rotated 180°, and the downward root growth measured every 4 d until Col-0 roots reached the bottom of the plate: 12 d on 0.5x MS media and 20 d on 0.5x MS supplemented with 75 mM NaCl.

To evaluate shoot development, four healthy 4-d-old seedlings, two of each genotype, were transferred into a Magenta box containing the same agar media as used for the root elongation experiments, with or without the addition of extra NaCl or other salts. The effects of salt stress were normally evaluated after 3-5 wk.

For root cortical cell size measurements, segments of differentiated roots maintained in liquid growth media were observed

under a microscope using Nomarski optics. Five different roots were sampled per genotype in each of three independent experiments.

GUS reporter construction and assay

The plasmid pAHA4::GUS was made to express the β -glucuronidase reporter from the *AHA4* promoter. A 2-kb Sall/XhoI fragment containing the promoter, 5' untranslated sequence and 39 bp of *AHA4* coding sequence was isolated from the *AHA4* genomic clone p74 and cloned into the Sall site of the transformation vector pBI101-1 (Clontech, Palo Alto, CA, USA). Transgenic plants expressing this construct were generated by a vacuum infiltration protocol (Bechtold *et al.*, 1993) using *Agrobacterium tumefaciens* strain GV3101. Primary transformants were selected on GM media containing kanamycin (50 mg l⁻¹) and carbenicillin (100 mg l⁻¹).

Histochemical analysis of GUS expression was done on S1 plants (self-fertilization of the primary transformants) and was verified in the S2 and S3 generations. Tissues were submersed in staining solution containing 0.5 mg ml⁻¹ of 5-bromo-4-chloro-3-indolyl β -D-glucuronide (X-gluc) in 100 mM Na-phosphate, pH 7.2, 10 mM EDTA, 0.1% Triton X-100, 0.1% Sarcosyl, 0.5 mM K₃Fe[CN]⁶, 0.5 mM K₄Fe[CN]⁶ and 10 mM 2-mercaptoethanol. Samples were placed briefly under vacuum and then incubated at 37°C for 4–24 h. Siliques were opened longitudinally and fixed in 0.3% paraformaldehyde in 100 mM Na-phosphate, pH 7.2, for 1 h and then washed in 100 mM Na-phosphate, pH 7.2, prior to submersion in the staining solution. After the reaction, tissues were cleared and then incubated in mounting medium (10% ethanol, 50% glycerol). For cross-sections, selected stained roots were fixed overnight at 4°C in 3% glutaraldehyde in 50 mM Na-phosphate, pH 7.2, prior to infiltration with warmed 50 mM Na-phosphate, pH 7.2 containing 4% agarose. Hand cross-sections were then performed on the agarose embedded roots using a razor blade.

For quantitative β -glucuronidase (GUS) activity assays, fresh plant material was ground to powder in liquid nitrogen and immediately mixed with extraction buffer (100 mM sodium phosphate, pH 7.2, 10 mM EDTA, 0.1% Triton X-100, 0.1% Sarcosyl 100 μ M, 10 mM 2-mercaptoethanol). Extracts were spun at 11 000 g at 4°C for 15 min 40 μ l of supernatant was assayed for GUS activity (Jefferson *et al.*, 1987). Fluorescence measurements were performed on a fluorescence spectrophotometer model F-2000 (Hitachi). Total protein concentration was determined by the Bradford assay (Bio-Rad, Hercules, CA, USA). GUS activity was normalized per μ g of protein in the extract.

Complementation assays

An 8-kb BamHI/NheI fragment containing the entire *AHA4* coding sequence flanked by 4.1 kb of 5' sequence and 580 bp of 3' sequence was introduced into the plant transformation vector pSPTV20 (P. Doerner, unpublished) which carries the polyadenylation site sequence of the nopaline synthase gene (pAnos) on one side of the polycloning site and the gene for phosphinothricin acetyl transferase (*bar*) as unique plant selectable marker. Construction intermediates involved the introduction of a unique cloning site Ascl into both the plant transformation vector pSPTV20 (using a polylinker HindIII/Ascl/XbaI) and the genomic clone p74 (by subcloning the BamHI/Sall genomic fragment into a modified pBluescript SK-containing an Ascl site added with a polylinker XbaI/Ascl/SacI). The Ascl/NheI fragment

from the intermediate genomic clone was cloned into the modified pSTV20 vector cut by Ascl and XbaI allowing the pAnos sequence to flank the 3' end of the inserted plant sequence. Transgenic *aha4-1* (E) plants were generated by a vacuum infiltration protocol using *Agrobacterium tumefaciens* strain GV3101. Primary transformants were selected on GM media containing phosphinotricine (50 mg l⁻¹) and carbenicillin (100 mg l⁻¹).

Elemental analysis

Analysis was performed on the leaves of Col-O and *aha4-1* plants transferred at the 4-d-old stage and grown on GM media containing 75 mM or 110 mM NaCl. Green rosette leaves well above the media were collected, weighed, and dried at 65°C for 48 h then weighed again. The samples were digested 1 h in 0.5 ml of 65% HNO₃ (metal free quality, Fisher Scientific, Pittsburgh, PA, USA) then overnight after a 1–1 dilution with double distilled water. Digested tissues were diluted to a final 3.25% HNO₃ prior to measuring. Potassium, Na, Ca, Mg, and P concentrations were determined by ICP-AES on a model Optima 3000XL (Perkin Elmer, Norwalk, CT, USA).

Reverse transcriptase-polymerase chain reactions

Total RNA was isolated by using the RNeasy Plant Mini Kit (Qiagen, Santa Clarita, CA, USA) and cDNA synthesized using the SuperScript preamplification system (GibcoBRL, Bethesda, MD, USA). 10–5% of the first strand reactions were used for PCR amplification with ExTaq polymerase (Panvera, Madison, WI, USA) following manufacturer instructions. Quantitative RT-PCR was performed as follows. Five to 10% of the same first strand cDNA reactions were used as templates in parallel 60 μ l PCR reactions with primers for either *AHA4*, eukaryotic initiation factor 4 α -2 (*eIF4 α -2*), or ubiquitin isoform 10 (*UBQ10*). Before starting the PCR reactions each 60 μ l mix was divided into 12 μ l aliquots allowing the reaction to be sampled after an increasing number of amplification cycles (typically 12, 14, 16, and 18). The amplified products were run on the same 0.8% agarose gel by reloading consecutively in the same wells the products obtained with the different set of primers. DNA was blotted onto a nylon membrane (Hybond N, Amersham, Arlington Heights, IL, USA) and hybridized against an excess of probes corresponding to the PCR products: 40 ng of ³²P-labeled probes added to 80 ng of cold probe for the *AHA4* product and 120 ng of cold products for the internal controls. Signal intensity was quantitated by phosphor-imaging analysis (Multi-Analysis system, BioRad, Hercules, CA, USA).

AHA4 specific primers were primer 139c 5'-CAAATTCTTCA-TCCGCTACG-3' and 144b, 5'-CTGACATGGGTTTCGATCTGTG-3'. *eIF4 α -2* primers were *eIF4 α -2u*, 5'-CTCTCGCAATCTTCGCTCT-TCTCTTT-3' and *eIF4 α -2d*, 5'-TTCTCAAACCATTAAGCATAAA-TACCC-3'. *UBQ10* primers were *UBQ10u*, 5'-CTCGTCTCTGT-TATGCTTAAG-3' and *UBQ10d*, 5'-GAAGAAGTTCGACTTGTC-3'.

Acknowledgements

We thank Takashi Araki, Sherry Kempin, and Martin Yanofsky for providing the *aha4-1* T-DNA line and for their contributions to its characterization. This research was supported by grants to J.F.H. from the US Department of Agriculture (92-37304-7889), Department of Energy (DE-FG03-94ER20152), a joint grant from

the National Aeronautics and Space Administration and National Science Foundation (IBN-9416038), a grant from the Human Frontiers Science Program (RG0268/2000-M), and support from the Novartis Agriculture Discovery Institute.

References

- Assmann, S.M.** (1993) Signal transduction in guard cells. *Annu. Rev. Cell Biol.* **9**, 345–375.
- Bechtold, N., Ellis, J. and Pelletier, G.** (1993) *In planta Agrobacterium* mediated gene transfer by infiltration of adult *Arabidopsis thaliana* plants. *C. R. Acad. Sci. Paris, Life Sci.* **316**, 1194–1199.
- Boutry, M., Michelet, B. and Goffeau, A.** (1989) Molecular cloning of a family of plant genes encoding a protein homologous to plasma membrane H⁺-translocating ATPases. *Biochem. Biophys. Res. Comm.* **162**, 567–574.
- Chadwick, C.C., Goormaghtigh, E. and Scarborough, G.A.** (1987) A hexameric form of the *Neurospora crassa* plasma membrane H⁺-ATPase. *Arch. of Biochem. & Biophys.* **252**, 348–356.
- De Michelis, M., Pugliarello, M., Rasi-Caldogno, F. and Soave, C.** (1996) A mutant of *Arabidopsis thaliana* partially resistant to fusaric acid has reduced plasma membrane H⁺-ATPase. *Plant Cell Env.* **19**, 362–366.
- Ewing, N.N., Wimmers, L.E., Meyer, D.J., Chetelat, R.T. and Bennett, A.B.** (1990) Molecular cloning of tomato plasma membrane H⁺-ATPase. *Plant Physiol.* **94**, 1874–1881.
- Geelen, D., Lurin, C., Bouchez, D., Frachisse, J.-M., Lelievre, F., Courtial, B., Barbier-Brygoo, H. and Maurel, C.** (2000) Disruption of putative anion channel gene AtCLC-a in *Arabidopsis* suggests a role in the regulation of nitrate content. *Plant J.* **21**, 259–267.
- Harper, J.F., Manney, L. and Sussman, M.** (1994) The plasma membrane H⁺-ATPase gene family in *Arabidopsis*; genomic sequence of AHA10 which is expressed primarily in developing seeds. *Mol. Gen. Genet.* **244**, 572–587.
- Jefferson, R.A.** (1987) Assaying chimeric genes in plants: The GUS gene fusion system. *Plant Molecular Biology Reporter*, **5**, 387–405.
- Krysan, P., Young, J., Tax, F. and Sussman, M.** (1996) Identification of transferred DNA insertions within *Arabidopsis* genes involved in signal transduction and ion transport. *Proc. Natl Acad. Sci. USA*, **93**, 8145–8150.
- Luo, H., Morsomme, P. and Boutry, M.** (1999) The two major types of plant plasma membrane H⁺-ATPases show different enzymatic properties and confer differential pH sensitivity of yeast growth. *Plant Physiol.* **119**, 627–634.
- Maldonado, A.M., de la Fuente, N. and Portillo, F.** (1998) Characterization of an allele-nonspecific intragenic suppressor in the yeast plasma membrane H⁺-ATPase gene (*Pma1*). *Genetics*, **150**, 11–19.
- Marre, M., Venegoni, A., Talarico, A., Soave, C. and Marre, E.** (1995) Evidence that the partial resistance of the *Arabidopsis* 5–2 mutant to fusaric acid depends on a decreased capacity of the H⁺ pump to respond to activating factors. *Plant Cell Env.* **18**, 651–659.
- Mathieu, Y., Jouanneau, J.P., Thomine, S., Lapous, D. and Guern, J.** (1994) Cytosolic protons as secondary messengers in elicitor-induced defence responses. *Biochem. Soc. Symposium*, **60**, 113–130.
- Michelet, B. and Boutry, M.** (1995) The plasma membrane H⁺-ATPase. *Plant Physiol.* **108**, 1–6.
- Moriau, L., Bogaerts, P., Jonniaux, J. and Boutry, M.** (1993) Identification and characterization of a second plasma membrane H⁺-ATPase gene subfamily in *Nicotiana plumbaginifolia*. *Plant Mol. Biol.* **21**, 955–963.
- Moriau, L., Michelet, B., Bogaerts, P., Lambert, L., Michel, A., Oufattole, M. and Boutry, M.** (1999) Expression analysis of two gene subfamilies encoding the plasma membrane H⁺-ATPase in *Nicotiana plumbaginifolia* reveals the major transport functions of this enzyme. *Plant J.* **19**, 31–41.
- Morsomme, P. and Boutry, M.** (2000) The plant membrane H⁺-ATPase: structure, function and regulation. *Biochim. Biophys. Acta*, **1465**, 1–16.
- Niu, X., Bressan, R., Hasegawa, P. and Pardo, J.** (1995) Ion homeostasis in NaCl stress environments. *Plant Physiol.* **109**, 735–742.
- Niu, X., Damsz, B., Kononowicz, A.K., Bressan, R.A. and Hasegawa, P.M.** (1996) Tissue specific induction of plasma membrane H⁺-ATPase gene expression by NaCl. *Plant Physiol.* **111**, 679–686.
- Niu, X., Narasimhan, M.L., Salzman, R.A., Bressan, R.A. and Hasegawa, P.M.** (1993) NaCl regulation of plasma membrane H⁺-ATPase gene expression in a glycophyte and halophyte. *Plant Physiol.* **103**, 713–718.
- Palmgren, M.G. and Christensen, G.** (1994) Functional comparisons between plant plasma membrane H⁺-ATPase isoforms expressed in yeast. *J. Biol. Chem.* **269**, 3027–3033.
- Pitman, M.G., Lauchli, A. and Stelzer, R.** (1981) Ion distribution in roots of barley seedlings measured by electron probe X-ray analysis. *Plant Physiol.* **68**, 673–679.
- Portillo, F.** (1997) Characterization of dominant lethal mutations in the yeast plasma membrane H⁺-ATPase gene. *FEBS Lett.* **402**, 136–140.
- Portillo, F.** (2000) Regulation of plasma membrane H⁺-ATPase in fungi and plants. *Biochim. Biophys. Acta*. **1469**, 31–42.
- Reuveni, M., Bressan, R.A. and Hasegawa, P.M.** (1993) Modification of proton transport kinetics of the plasma membrane H⁺-ATPase after adaptation of tobacco cells to NaCl. *J. Plant Physiol.* **142**, 312–318.
- Scarborough, G.A.** (2000) Crystallization, structure and dynamics of the proton-translocating P-type ATPase. *J. Exp. Biology*, **203**, 147–154.
- Serrano, R.** (1996) Salt tolerance in plants and microorganisms: toxicity targets and defence responses. *Intern. Rev. Cytol.* **165**, 1–52.
- Serrano, R., Kielland-Brandt, M. and Fink, G.** (1986) Yeast plasma membrane ATPase is essential for growth and has homology with (Na⁺K⁺), K⁺ and Ca²⁺-ATPases. *Nature*, **319**, 689–693.
- Vallejo, C. and Serrano, R.** (1989) Physiology of mutants with reduced expression of plasma membrane H⁺-ATPases. *Yeast*, **5**, 307–319.
- Wu, S.-J., Ding, L. and Zhu, J.-K.** (1996) SOS1, a genetic locus essential for salt tolerance and potassium acquisition. *Plant Cell*, **8**, 617–627.
- Zhao, R., Dielen, V., Kinet, J.-M. and Boutry, M.** (2000) Cossuppression of a plasma membrane H⁺-ATPase isoform impairs sucrose translocation, stomatal opening, plant growth, and male fertility. *Plant Cell*, **12**, 535–546.